Polarization anisotropy in resonant x-ray emission from molecules

Yi Luo, Hans Ågren, and Faris Gel'mukhanov*
Institute of Physics and Measurement Technology, Linköping University, S-58183, Linköping, Sweden
(Received 1 September 1995)

We investigate the polarization anisotropy of resonant x-ray emission using one-step, two-step, and classical formulations. It is shown, analytically and numerically, that these models in general give different polarization anisotropies. We compare also the results of the one- and two-step models for the integrated unpolarized cross sections over the same set of test molecules. These include two of the chlorofluoromethanes used originally to experimentally verify the polarization anisotropy in resonant x-ray emission. The test molecules also represent species with core-level chemical shifts and species with symmetry-adapted and quasidegenerate core levels. It is shown that only in the case of energy-isolated and localized symmetry-non-adapted core levels do the two-step model and the — in that case identical—classical model apply, while in all other cases, the one-step model is required either for the polarization anisotropy or for the total cross section, or for both these quantities.

PACS number(s): 33.70.−w, 33.20.Rm

I. INTRODUCTION

Improvements in construction principles of high brightness synchrotron radiation sources, x-ray monochromators, and x-ray spectrometers have resurged the interest in resonant x-ray scattering measurements. The ability to generate x-ray emission spectra by selective excitation involving discrete core-excited states has made it possible to record fluorescence spectra covering a large interval in the x-ray wavelength region [1–5]. A distinct step forward in this field was obtained in the works of Lindle and co-workers [2–4], in which it was shown that the polarization of $K\beta$ fluorescence x-ray spectra of chlorofluoromethanes is strongly anisotropic. It was found that the degree and the direction of the x-ray polarization is dependent on both the energy of excitation and the symmetry of the involved molecular valence orbitals.

The experimental development has to some extent been matched by new theoretical modeling of the x-ray scattering process. The concept of directional preparation of resonant x-ray emission [6] was, however, introduced already 20 years ago, long before the modern experiments, and stood then in some contrast to the attempts to explain polarization anisotropy by stochastic methods. Using this concept, the polarization of the exciting beam ''lines up'' the target molecules with an anisotropy that is determined by the orientation of the polarization vector with respect to the transition dipole moment. This anisotropy in turn determines the polarization direction of the emission. Thus, even if the target molecules are randomly oriented, the directional preparation leads to strong polarization anisotropy when the resonant and final-state levels contain elements of symmetry.

A general theory of symmetry and polarization resonant x-ray scattering (RXS) (inelastic and elastic) has now been derived with cross-section formulas uncovering the polarization, orientation, and symmetry dependencies that apply to any molecule using arbitrary types of polarized radiation [7,8]. By performing orientational averaging, pertinent to RXS spectra of gas phase molecules, this formulation can in principle be used to derive symmetries of occupied and unoccupied molecular orbitals from various measured polarization ratios (ratios of cross sections for different combinations of polarization directions of incoming and outgoing x-ray photons). However, except for the works of Lindle and coworkers [2–4] using the classical formula and for the work on polarization distributions for resonant x-ray spectra of H_2S in the *elastic* mode [9], no quantitative analysis of the polarization anisotropy in resonant x-ray emission experiments of randomly oriented systems have, to our knowledge, been undertaken. In particular, there is need to systematically explore the limitations of either the classical formula as originally used in Refs. [3,4] or the two-step formulas in light of the general one-step formulation of the symmetry and polarization selective RXS process [7,8], because these models provide a simpler interpretation of the experiments. The present work intends to use a set of representative cases to do just that. Except for the chlorofluoromethanes, we include aniline as representing the common case of chemically shifted core levels and C_{60} representing symmetry-adapted and quasidegenerate core levels.

II. THEORY FOR POLARIZED RESONANT X-RAY EMISSION FROM MOLECULES

It is generally agreed that resonant x-ray emission spectra of molecules are adequately represented by a one-step model describing resonant x-ray inelastic scattering as one process. Several different features of resonant x-ray emission spectra have been obtained from this model [8,10–12]. The popularity of the two-step model stems from its simplicity and from its applicability to nonresonant x-ray emission. For resonant emission it is, however, necessary for each given case to inspect the applicability of the this model and to explore its overlap with the one-step model. A problem for such an investigation is that, in contrast to the one-step model, there is no consistent definition of a two-step model. As an alternative to the customary two-step model we investigate here also a more general two-step model.

*Permanent address: Institute of Automation and Electrometry, 630090 Novosibirsk, Russia.

A. The one-step model

The cross section of resonant x-ray inelastic scattering (RIXS) for a realistic experimental situation can be expressed as [7,10,11]

$$\sigma(\omega',\omega_0)=\sum_{\nu,n}\frac{\omega'}{\omega}|F_{\nu n}(\omega)|^2\Phi(\omega'+\omega_{\nu n}-\omega_0), \quad (1)$$

where $\Phi(\omega-\omega_0)$ in the incoming photon distribution function centered at frequency ω_0. The frequency ω' of the emitted x-ray photons has a Raman related shift (Stokes shift) into the long-wavelength region relative to the frequency ω of the absorbed photon

$$\omega=\omega'+\omega_{\nu n}, \quad (2)$$

in accordance with the energy conservation law reflected by the $\delta(\omega-\omega'-\omega_{\nu n})$ function. $|F_{\nu n}(\omega)|$ is the Kramers-Heisenberg formula for the resonant x-ray scattering amplitude [13,14]

$$F_{\nu n}(\omega)=\sum_k f^k_{\nu n}(\omega), \quad (3)$$

$$f^k_{\nu n}(\omega)=\alpha\omega_{\nu k}\omega_{nk}(\nu)\frac{(\mathbf{e}_1^*\cdot\mathbf{d}_{\nu k})[\mathbf{e}_2\cdot\mathbf{d}_{kn}(\nu)]}{\omega-\omega_{\nu k}+i\Gamma_{\nu k}}, \quad (4)$$

where $f^k_{\nu n}(\omega)$ denotes the partial or channel amplitude of the RIXS process. The kth channel amplitude $f^k_{\nu n}(\omega)$ describes the two-photon process of absorption of incoming and emission of final x-ray photons, the frequencies and polarization vectors of which are $\omega\omega'$ and $\mathbf{e}_1,\mathbf{e}_2$, respectively. The polarization vectors are in laboratory coordinates X,Y, and Z. The index k enumerates localized or delocalized core orbitals ψ_k. We use atomic units (h=m=e=1, $\alpha=\frac{1}{137}$) and the following notations: $\omega_{\nu k}=E(k^{-1}\nu)-E_0,\omega_{nk}(\nu)=E(k^{-1}\nu)-E(n^{-1}\nu),\mathbf{d}_{\nu k}=\langle 0|\mathbf{d}|k^{-1}\nu\rangle$ and $\mathbf{d}_{kn}(\nu)=\langle k^{-1}\nu|\mathbf{d}|n^{-1}\nu\rangle$ are resonant frequencies and dipole matrix elements of x-ray absorption ($k\rightarrow\nu$) and emission ($n\rightarrow k$) transitions, respectively, where dipole matrix elements are expressed in molecular coordinates $\xi\eta$, and ζ. $\omega_{\nu n}=E(n^{-1}\nu)-E_0$ is a frequency for the optical excitation $n\rightarrow\nu$ and is equal to the difference between energies $E(n^{-1}\nu)$ and E_0 of excited $|n^{-1}\nu\rangle$ and ground $|0\rangle$ molecular states; $\Gamma_{\nu k}$ is the half-width at half maximum of the x-ray absorption line $k\rightarrow\nu$. The electron excited to the vacant molecular orbital (MO) ψ_ν screens differently the subsequent decay of electrons from various occupied levels n to the inner shell k. This specific screening effect leads to a dependence on ν of the frequencies $\omega_{nk}(\nu)$ and the dipole matrix elements $\mathbf{d}_{kn}(\nu)$. The range of validity of the Kramers-Heisenberg formula (3) has recently been discussed in Ref. [7].

For the randomly oriented gas or solvent molecules, orientational averaging should be conducted. A detailed description of this referring to the case of randomly oriented molecules can be found in our previous study [8] (see also work of McClain [15] for general two-photon transitions). It gives

$$\langle|F_{\nu n}|^2\rangle-\lambda_{\nu n}=F\lambda^F_{\nu n}+G\lambda^G_{\nu n}+H\lambda^H_{\nu n} \quad (5)$$

with

$$\lambda^F_{\nu n}=\sum_\beta F^{\beta\beta}_{\nu n}\sum_\gamma F^{\gamma\gamma *}_{\nu n}=\left|\sum_k \zeta^k_{\nu n}\cos\varphi^{kk}_{\nu n}\right|^2, \quad (6)$$

$$\lambda^G_{\nu n}=\sum_{\beta\gamma} F^{\beta,\gamma}_{\nu n}F^{\beta,\gamma *}_{\nu n}=\sum_{k,k_1}\zeta^{k*}_{\nu n}\zeta^{k_1}_{\nu n}\cos\varphi^{kk_1}_{\nu\nu}\cos\varphi^{kk_1}_{nn}, \quad (7)$$

$$\lambda^H_{\nu n}=\sum_{\beta,\gamma} F^{\beta,\gamma}_{\nu n}F^{\beta,\gamma *}_{\nu n}=\sum_{k,k_1}\zeta^{k*}_{\nu n}\zeta^{k_1}_{\nu n}\cos\varphi^{kk_1}_{\nu\nu}\cos\varphi^{k_1k}_{\nu n}. \quad (8)$$

The λ functions are expressed through the angle $\varphi^{kk_1}_{ij}$ between transition dipole moments $\mathbf{d}_{ik}$ and $\mathbf{d}_{jk_1}$

$$\cos\varphi^{kk_1}_{ij}=\frac{\mathbf{d}_{ik}\cdot\mathbf{d}_{jk_1}}{d_{ik}d_{jk_1}} \quad (9)$$

for the case of real dipole moments. Here

$$\zeta^k_{\nu n}=\frac{\alpha\omega_{\nu k}\omega_{nk}(\nu)}{\omega'-\omega_{nk}+i\Gamma_{\nu k}}d_{\nu k}d_{kn}. \quad (10)$$

The cross terms $\zeta^{k*}_{\nu n}\zeta^k_{\nu n}$ in Eqs. (6)–(8) describe the interference of scattering channels through the different core levels $k\neq k_1$. This interference is a characteristic feature of the one-step description, but is neglected in the two-step model. Further discussions on the difference between one- and two-step models are given in Sec. II C. The F, G, and H factors are

$$F=-|\mathbf{e}_1\cdot\mathbf{e}_2|^2+4|\mathbf{e}_1^*\cdot\mathbf{e}_2|^2-1, \quad (11)$$

$$G=-|\mathbf{e}_1\cdot\mathbf{e}_2|^2-|\mathbf{e}_1^*\cdot\mathbf{e}_2|^2+4, \quad (12)$$

$$H=4|\mathbf{e}_1\cdot\mathbf{e}_2|^2-|\mathbf{e}_1^*\cdot\mathbf{e}_2|^2-1. \quad (13)$$

The averaged cross section is given in terms of these factors as

$$\begin{aligned}\langle\sigma(\omega',\omega_0)\rangle&=\sum_{\nu,n}\frac{\omega'}{\omega}\lambda_{\nu n}\Phi(\omega'+\omega_{\nu n}-\omega_0)\\&=\sum_{\nu,n}\frac{\omega'}{\omega}(F\lambda^F_{\nu n}+G\lambda^G_{\nu n}+H\lambda^H_{\nu n})\\&\quad\times\Phi(\omega'+\omega_{\nu n}-\omega_0). \quad (14)\end{aligned}$$

These expressions show that the RIXS cross section in general depends strongly on the polarization vectors of absorbed and emitted photons and on the symmetries of the unoccupied and occupied MOs. Equation (14) is perfectly general for photons of any polarization: linear, circular, or elliptical.

It has been shown in our previous studies [8,16] how this formulation can be used for assigning the molecular orbitals from the polarization and symmetry dependencies of RIXS. For a detailed analysis on this aspect we refer to Ref. [8].

B. Two-step models

The traditional two-step formulation, which assumes the x-ray emission to be decoupled from the x-ray absorption

process, is known to be applicable in the nonresonant case far from threshold. Its limits, however, have not been investigated for the polarization anisotropy for near-threshold excitation in the region where resonant processes operate. The customary two-step model seems to be the one in which only emission transitions $W^E_{nk}(\omega')$ are taken into account:

$$\sigma^{\mathrm{TS1}}(\omega',\omega)\propto W^A(\omega)\sum_{k,n} W^E_{nk}(\omega')\propto\sum_{k,n} W^E_{nk}(\omega'). \tag{15}$$

This simple two-step model TS1 does not consider symmetry or polarization of excitation and can therefore evidently not be generally valid in the resonant case. In the following, we will only discuss the differences between the one-step model and a more general two-step model TS2. In this two-step model the resonant x-ray scattering cross section is proportional to the product of the absorption and emission probabilities $W^A_{k\nu}(\omega)$ and $W^E_{n,k}(\omega')$. This two-step model is then defined as

$$\sigma^{\mathrm{TS2}}(\omega',\omega)\propto\sum_{k,\nu} W^A_{k\nu}(\omega)\sum_{n} W^E_{n,k}(\omega'), \tag{16}$$

where

$$W^A_{k\nu}(\omega)=|\mathbf{e}\cdot\mathbf{d}_{\nu k}|^2\Delta(\omega-\omega_{\nu k},\Gamma_{\nu k}),$$

$$W^E_{nk}(\omega')=|\mathbf{e}'\cdot\mathbf{d}_{nk}|^2\Delta(\omega'-\omega_{nk},\Gamma_{nk}). \tag{17}$$

The TS1 and TS2 models will be the same when the absorption probability $W^A(\omega)=W^A_{k\nu}(\omega)$ is constant, for example, when ω exceeds the core ionization potential. Equation (15) is thus used for the calculation of the nonresonant x-ray emission spectra.

For the TS2 model a general formula for the randomly oriented molecules is obtained by orientational averaging. It gives

$$\langle\sigma^{\mathrm{TS2}}(\omega',\omega_0)\rangle\propto\sum_{\nu,n}[(F+H)\lambda^{\mathrm{TS2}}_{\nu n}+G\tilde{\lambda}^{\mathrm{TS2}}_{\nu n}]\times\Delta(\omega-\omega_{\nu k},\Gamma_{\nu k}), \tag{18}$$

where

$$\lambda^{\mathrm{TS}}_{\nu n}=\sum_k|\zeta^k_{\nu n}\cos\varphi^{kk}_{\nu,n}|^2,$$

$$\tilde{\lambda}^{\mathrm{TS}}_{\nu n}=\sum_k|\zeta^k_{\nu n}|^2. \tag{19}$$

The parameters F, H, and G are the same as in Eq. (13) and $\zeta^k_{\nu n}$ is defined by Eq. (10). The parameters $\lambda^{\mathrm{TS}}_{\nu n}$ and $\lambda^{G}_{\nu n}$ can be obtained from Eqs. (6)–(8) of the one-step model by only considering the direct terms ($k=k_1$). In the following we list the main distinctions between the two-step [Eq. (18)] and the one-step [Eqs. (1) and (14)] models.

C. Comparison between one- and two-step models

The polarization and angular dependencies of resonant x-ray fluorescence are also model sensitive. The one-step description yields qualitatively different polarization features in comparison with the two-step model. In the framework of this model [10] it was shown by one of us [6] that x-ray fluorescence from gas-phase molecules is strongly anisotropic, polarized, and state dependent if the incoming photon frequency ω is below or somewhat above the absorption threshold. This threshold effect was later observed in Cl and S K x-ray fluorescence of the gas-phase CH_3Cl [17], CF_3Cl [3], and H_2S [2] molecules. The effect can be explained qualitatively by the fact that a photoexcitation process near the threshold of anisotropic molecules is anisotropic and determined by the mutual orientation of the polarization vector $\mathbf{e}_1$ and the transition dipole moment $\mathbf{d}_{\nu k}$. Indeed, the absorption probability is $W^A_{k\nu}(\omega)\propto|\mathbf{e}\cdot\mathbf{d}_{\nu k}|^2$. So only molecules with $\mathbf{d}_{\nu k}$ parallel to $\mathbf{e}_1$ are excited. The excited molecules have certain space orientations because the orientation of $\mathbf{d}_{\nu k}$ is defined one to one by the molecular axis orientation and the symmetry of the unoccupied MO ψ_ν. Thus, like crystals, the space-oriented core-excited molecules emit polarized x-ray photons anisotropically.

For the case that the linear polarization vectors of absorbed and emitted photons have an angle θ, the polarization dependence of the intensity of the emitted photons $I(\theta)\propto\langle\sigma(\omega',\omega_0)\rangle$ can be expressed with help of Eq. (14) as

$$I(\theta)=I_0[1+R(3\cos^2\theta-1)], \tag{20}$$

where I_0 is proportional to the total intensity emitted in all directions and summed over all polarization vectors and R is the polarization anisotropy. For experimental reasons the polarization of both incoming and outgoing photons are seldom determined (see, however, experiments by Lindle *et al.* [17] and Southworth *et al.* [3]), and the cross section is obtained either as angular dependent for unpolarized incoming photons or as dependent on the polarization of the incoming photons for a fixed exit angle. It is necessary to replace $\cos^2\theta$ with $\frac{1}{2}\sin^2\chi$ for the two latter situations, i.e., when the initial x-ray beam is unpolarized or when a summation over the final photon polarization vectors $\mathbf{e}'$ is made. In the first case χ is the angle between $\mathbf{e}'$ and the direction $\mathbf{n}$ of incoming photon propagation; in the second case χ is the angle between $\mathbf{e}$ and $\mathbf{n}'$, the direction of the outgoing photon propagation. In this case, the Eq. (20) can be written as

$$I(\chi)=I_\perp(\chi)+I_\parallel(\chi),$$

$$I_\perp(\chi)=\tfrac{1}{2}I_0[1-R], \tag{21}$$

$$I_\parallel(\chi)=\tfrac{1}{2}I_0[1+R(3\sin^2\chi-1)].$$

Using a special spectrometer, it is then possible to measure the two different components $I_\perp$ and $I_\parallel$ as done by Lindle *et al.* [17] and Southworth *et al.* [3]. It thus provides the same information as Eq. (20).

From the one-step model (OSM), Eq. (14), the polarization anisotropy parameter R can be determined as

$$R^{\mathrm{OSM}}=\frac{1}{5}\left[\frac{3\sum_{\nu,n}(\lambda^{F}_{\nu n}+\lambda^{H}_{\nu n})\Phi(\omega'+\omega_{\nu n}-\omega_0)}{2\sum_{\nu,n}\lambda_{\nu n}\Phi(\omega'+\omega_{\nu n}-\omega_0)}-1\right] \tag{22}$$

and the intensity I_0 expressed as

$$I_0^{\mathrm{OSM}}=\tfrac{10}{3}\sum_{\nu,n}\frac{\omega'}{\omega}\lambda^{G}_{\nu n}\Phi(\omega'+\omega_{\nu n}-\omega_0). \tag{23}$$

To see the difference between the two-step and one-step models we give the expression for R and I_0 for the two-step model neglecting interference. We then take into account the two-step model expressions Eqs. (19) and (20):

$$R^{\mathrm{TS2}}=\tfrac{1}{5}(3\overline{\cos^2\varphi}-1). \tag{24}$$

The polarization anisotropy parameter R in the two-step model is determined by averaging the angle φ between absorption and emission dipole moments

$$\overline{\cos^2\varphi}=\frac{\sum_{\nu,n,k}\eta^{k}_{\nu n}\cos^2\varphi^{kk}_{\nu n}}{\sum_{\nu,n,k}\eta^{k}_{\nu n}}. \tag{25}$$

The parameter $\eta^{k}_{\nu n}$ reflects the contribution of the scattering channel $(k\rightarrow\nu,\ n\rightarrow k)$ to the x-ray fluorescence intensity

$$\eta^{k}_{\nu n}=\xi^{k}_{\nu n}\Delta(\omega-\omega_{\nu k},\Gamma_{\nu k}). \tag{26}$$

The intensity I_0 is given by

$$I_0^{\mathrm{TS2}}=\tfrac{10}{3}\sum_{\nu,n,k}\eta^{k}_{\nu n}. \tag{27}$$

The classical formula for the polarization anisotropy parameter is valid only when one scattering channel $(k\rightarrow\nu,\ n\rightarrow k)$ predominates

$$R^{\mathrm{class}}=\tfrac{1}{5}(3\cos^2\varphi-1), \tag{28}$$

where $\varphi\equiv\varphi^{kk}_{\nu n}$ is the angle between the dipole moments of absorption and emission transitions $\mathbf{d}_{\nu k}$ and $\mathbf{d}_{kn}$. The two-step model for the average angle between absorption and emission dipole moments [Eq. (25)] is an obvious generalization of the classical angle $\varphi\equiv\varphi^{kk}_{\nu n}$. A comparison of the two-step result Eq. (24) with the explicit one-step formula Eq. (22) [see also Eqs. (6)–(8) and (14)] shows the strong influence of interference of scattering channels on the polarization of x-ray fluorescence. The channel interference is reflected in Eqs. (6)–(8) by the cross terms $(k\neq k_1)$ under summation over core levels k. In many cases, as for the C_{60} molecule used as an example below, the core orbitals are strongly degenerate. Therefore, the contribution to the cross section and to the polarization anisotropy parameter of the interference terms $(k\neq k_1)$ are comparable with the direct or two-step model terms $(k=k_1)$. Also, the total unpolarized cross section [see Eq. (20)] is subject to interference effects that distinguish the one-step from the two-step model in which the x-ray scattering cross section for a given channel [Eq. (16)] is assumed to be proportional to both the absorption and emission probabilities.

The significance of the interference effects can be illustrated even for a system with only two possible channels, i.e., for the case where there are only two core orbitals (k_1,k_2), involved in the process. Considering the case with only one valence orbital n and one unoccupied orbital ν, the one-step model gives

$$I_0^{\mathrm{OSM}}\propto\lambda^{G}_{\nu n}=I_1+I_2+I_{\mathrm{cross}} \tag{29}$$

and

$$I_1=|\zeta^{k_1}_{\nu n}|^2,\quad I_2=|\zeta^{k_2}_{\nu n}|^2,$$

$$I_{\mathrm{cross}}=2\,\mathrm{Re}(\zeta^{k_1*}_{\nu n}\zeta^{k_2}_{\nu n})\cos\varphi^{k_1k_2}_{\nu\nu}\cos\varphi^{k_1k_2}_{nn}. \tag{30}$$

According to the general two-step model TS2, the emission intensity is

$$I_0^{\mathrm{TS2}}\propto I_1+I_2. \tag{31}$$

To rewrite Eq. (30) one has

$$I_0^{\mathrm{OSM}}\propto I_0^{\mathrm{TS2}}(1+I_{\mathrm{int}}) \tag{32}$$

and

$$I_{\mathrm{int}}=I_{\mathrm{cross}}/I_0^{\mathrm{TS2}}=\frac{2\,\mathrm{Re}(\zeta^{k_1*}_{\nu n}\zeta^{k_2}_{\nu n})\cos\varphi^{k_1k_2}_{\nu\nu}\cos\varphi^{k_1k_2}_{nn}}{|\zeta^{k_1}_{\nu n}|^2+|\zeta^{k_2}_{\nu n}|^2}. \tag{33}$$

The difference between the one-step and the two-step models is thus dependent on the interference strength I_{int}, $0\leqslant|I_{\mathrm{int}}|\leqslant1$. If the interference strength is equal to zero, both models will give the same result; when the interference strength is equal to -1 the spectral line is depleted.

The difference between σ^{TS2} and σ^{OSM} is obvious, and it is quite evident that the two-step model cannot give a quantitative description for a process that contains more than one core-excited state, as will be further shown below. Other distinctions between the one-and two-step models emerge because absorption $W^{A}_{k\nu}(\omega)$ and emission $W^{E}_{nk}(\omega')$ probabilities are strongly coupled in the latter description by the energy conservation law Eq. (2), as reflected by the Dirac Δ function $\delta(\omega-\omega'-\omega_{\nu n})$ when $\Gamma_{\nu n}\ll\Gamma_{nk}$ [7]. This leads to experimentally observable effects [12,18] such as resonance narrowing, Raman related shifts, and Stokes doubling. Energy conservation can of course *ad hoc* be imposed also on the two-step formula, but does not enter in the description of RXS as naturally as in the one-step case.

III. MODEL CALCULATIONS

We carry out model calculations for a set of molecules in order to explore the differences between one- and two-step models for polarized resonant x-ray emission spectra. Apart from the polarization anisotropy (R), we investigate the nonpolarized intensity (I_0), and both these quantities will be the subject for the discussion presented in the following subsections. All calculations are performed at the frozen Hartree-

Fock level with double-zeta basis sets (based on test calculations on RIXS spectra given in Refs. [16,19]; the computational details are insignificant for the present findings). Only the case when the excitation energy is resonant with the first core-excited state is considered. The lifetimes of the core excited states of C and Cl are set to 0.15 and 0.6 eV, respectively. The linewidths of incoming photons are assumed to be 0.2 eV for C $K\alpha$ emission and 0.9 eV for Cl $K\beta$ emission, respectively. Since the linewidths of incoming photons are larger than the lifetime widths the effects of resonant narrowing on the polarization anisotropy is not discussed.

A. CF_3Cl

A comprehensive experimental analysis on the resonant Cl $K\beta$ emission spectra of CF_3Cl has been provided by Southworth *et al.* [3]. These authors found that the classical formula for the polarization anisotropy works quite well for this molecule. As shown in Sec. II C, the one-step, two-step, and classical models give the same predictions when there is only one core hole involved in the scattering. Figure 1 shows the calculated unpolarized intensity I_0 and polarization anisotropy parameter R for the case when the core orbital $1a_1$, Cl(1s), is resonantly excited to the lowest unoccupied molecular orbital (LUMO) $11a_1$. Applying the classical formula Eq. (28), one obtains $R(a_1)=\frac{2}{5}$ and $R(e)=-\frac{1}{5}$, which are the same as the experimental measurements.

We find $I_0(10a_1):I_0(7e)=0.24$, where the experimental measurement gives $I_0(10a_1):I_0(7e)=0.14$ [3]. This difference is purely due to the limitation of the computation, but not the choice of models. Without considering screening, one obtains from either the one- or the two-step models that

$$I_{\text{non}}(10a_1):I_{\text{non}}(7e)=I_0(10a_1):I_0(7e)=0.24, \qquad (34)$$

which is in good agreement with the nonresonant experimental value of 0.27 [20]. Screening leads to a dependence on ν of the emission energy $\omega_{nk}(\nu)$ and the dipole matrix elements $\mathbf{d}_{kn}(\nu)$ and Eq. (34) will no longer hold. Experimentally it is found that screening causes an energy shift up to 1.0 eV [21]. The difference between calculated and experimental values for $I_0(10a_1):I_0(7e)$ might indicate screening effects on the dipole matrix elements.

B. CF_2Cl_2

The polarization dependence of resonant x-ray emission spectra for the CF_2Cl_2 molecule has been observed experimentally, but without further interpretation [4]. Having only two symmetry-related atoms involved in the x-ray emission, this molecule poses a good test case for the investigation of the difference between one- and two-step models.

The relevant LUMO level is assigned as $13a_1$ [20]. The two Cl 1s core orbitals have the symmetries a_1 and b_2, which are both dipole allowed in transitions to the LUMO. There are therefore two close-lying core-excited states involved in the resonant x-ray emission and one thus expects to observe some differences between the one- and two-step models. Figure 2 shows the unpolarized intensity I_0 and polarization anisotropy R calculated by the one- and two-step models. A quite large difference for the polarization anisotropy R between the two models is observed, while they give the same results for the intensity distribution for the unpolarized intensity I_0. This can be understood by inspection of the formula for I_0 and R. As shown in Eq. (23), the unpolarized intensity I_0 is in the one-step model determined by the parameter $\lambda^G_{\nu n}$. According to Eq. (7), one can see that for a molecule belonging to the C_{2v} point group

$$\cos\varphi^{kk_1}_{aa}=\begin{cases}1 \text{ if } k \text{ and } k_1 \text{ have the same symmetry}\\ 0 \text{ if } k \text{ and } k_1 \text{ have different symmetry,}\end{cases} \qquad (35)$$

where a refers either to the valence orbital n or to the unoccupied orbital ν. In the case of the CF_2Cl_2 molecule, the two Cl 1s core orbitals have different symmetries and the

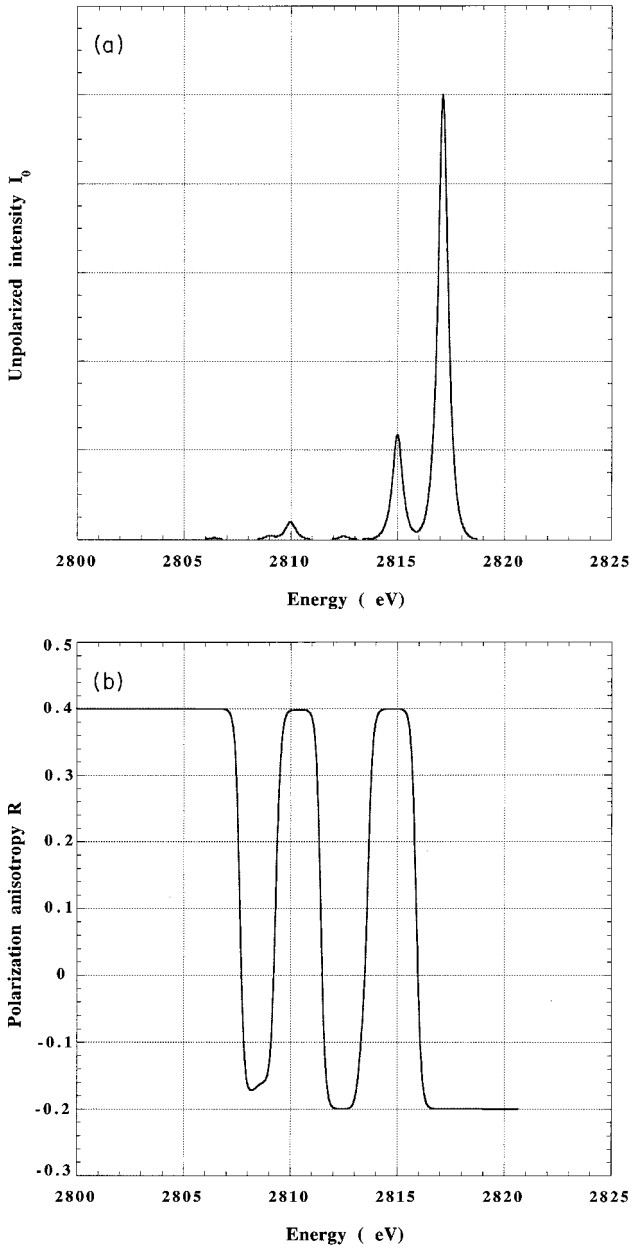

FIG. 1. (a) Unpolarized intensity I_0 and (b) polarization anisotropy parameter R for the CF_3Cl molecule.

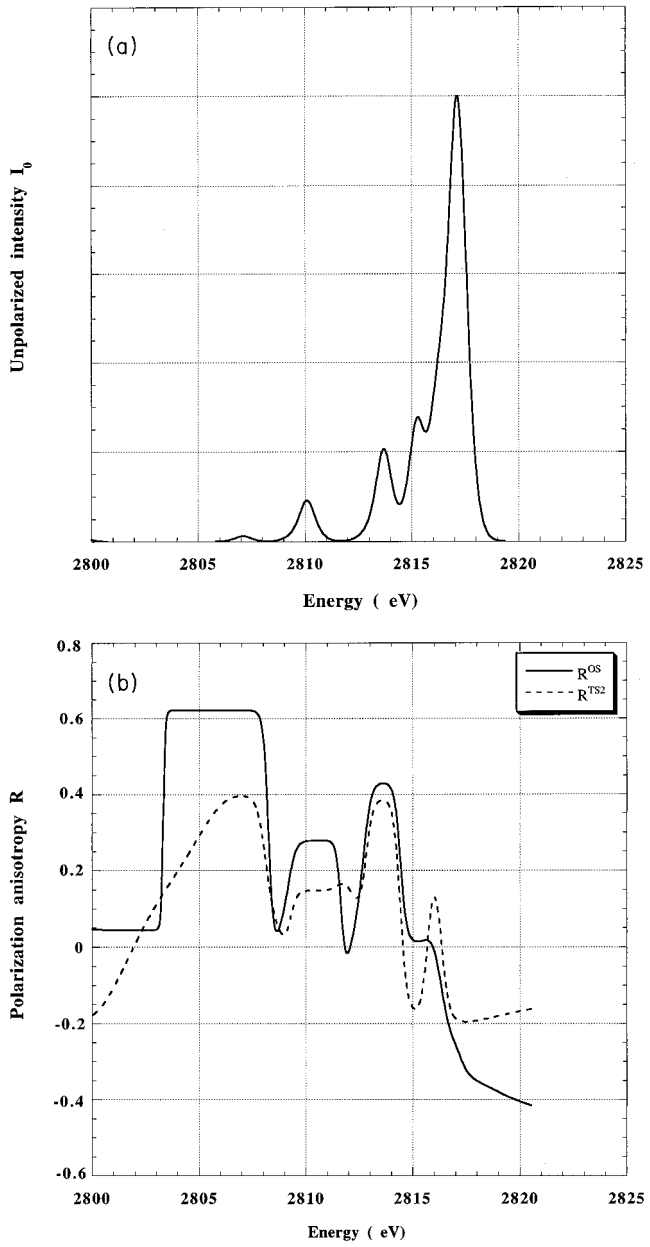

FIG. 2. (a) Unpolarized intensity I_0 and (b) polarization anisotropy parameter R for the CF_2Cl_2 molecule, calculated by one-step (solid line) and two-step (dashed line) models.

contribution from the interference terms for the unpolarized intensity I_0 is zero. The one- and two-step models should thus give the same result for the intensity distribution of I_0. However, for the polarization anisotropy parameter R, there is another type of interference term $\cos\varphi_{\nu n}^{kk_1}$ associated with the parameter $\lambda_{\nu n}^{H}$ see Eqs. (8) and (22). No simple relation like Eq. (35) can be obtained for this term. For the case studied here, where the symmetries of the core orbitals and the unoccupied orbital are known, the interference effect can be directly related to the symmetries of the valence orbitals n. Such an interference effect is responsible for the differences shown in Fig. 2(b).

C. $C_6H_5(NH_2)$

Like other monosubstituted benzenes, the aniline (aminobenzene) molecule provides a good test case for the role of chemical shifts in x-ray spectra [22]. It has been found that for the spectrum referring to the first strong π^* resonance of this molecule, three different channels, namely, the transitions from the $C_{2,3,4}(a_1)$ core orbitals to the first $\pi^*(b_1)$ molecular orbital, should be taken into account [22], while the second absorption feature can be assigned as one separate transition to the π^* level from the distinctly shifted core level associated with the carbon atom closest to the amino group [see Fig. 3(a)]. The latter represents the same case with isolated core levels as does CF_3Cl treated in Sec. III A above, thus with the two-step model description being appropriate for both the polarization anisotropy and the integrated cross section. The three intermediate core-excited states, especially $C_3(a_1)\pi^*(b_1)$ and $C_2(a_1)\pi^*(b_1)$, pose a more interesting case because of their small energy separations, and one can anticipate large interference effects as discussed in Sec. II C. The calculated unpolarized intensity I_0 and the polarization anisotropy R are shown in Fig. 3. In contrast to the case of CF_2Cl_2, the unpolarized intensities I_0 from the two models now show different intensity distributions. The spectrum calculated from the one-step model gives good agreement with the experimental observation. On the other hand, the polarization anisotropy R shows the same behavior for both models. This is easy to understand following the same discussion as in Sec. III B. We know from Eq. (35) that when the core orbitals have the same symmetry, the interference terms will contribute to the unpolarized intensity I_0. It is this interference effect that makes the difference between the one- and two-step models shown in Fig. 3(b). In the two-step model the polarization anisotropy R has a simple form for low symmetry point groups, i.e., for C_{2v}

$$R^{\mathrm{TS2}}=\begin{cases}2/5 & \text{if } \nu \text{ and } n \text{ have the same symmetry}\\ -1/5 & \text{if } \nu \text{ and } n \text{ have different symmetry.}\end{cases} \tag{36}$$

This could be directly obtained from Eqs. (24) and (25). By inspecting Eqs. (6)–(8), one finds that the one-step model gives

$$\lambda_{\nu n}^{F}=\lambda_{\nu n}^{H}=\begin{cases}\lambda_{\nu n}^{G} & \text{if } \nu \text{ and } n \text{ have the same symmetry}\\ 0 & \text{if } \nu \text{ and } n \text{ have different symmetry,}\end{cases} \tag{37}$$

where one should keep in mind that the core orbitals have the same symmetry. Putting Eq. (37) into Eq. (22), the same relation as shown in Eq. (36) for the two-step model is obtained for the one-step model as well.

D. C_{60}

Being of high, isocahedral, symmetry C_{60} served as an illustration for the symmetry selective character of RXS for randomly oriented molecules [16]. Here we compare differences between the one- and two-step models with respect to intensities and polarization of the RIXS spectra of this high-symmetry molecule. We explore the case when the energy of incoming photons is resonant with the first isolated LUMO

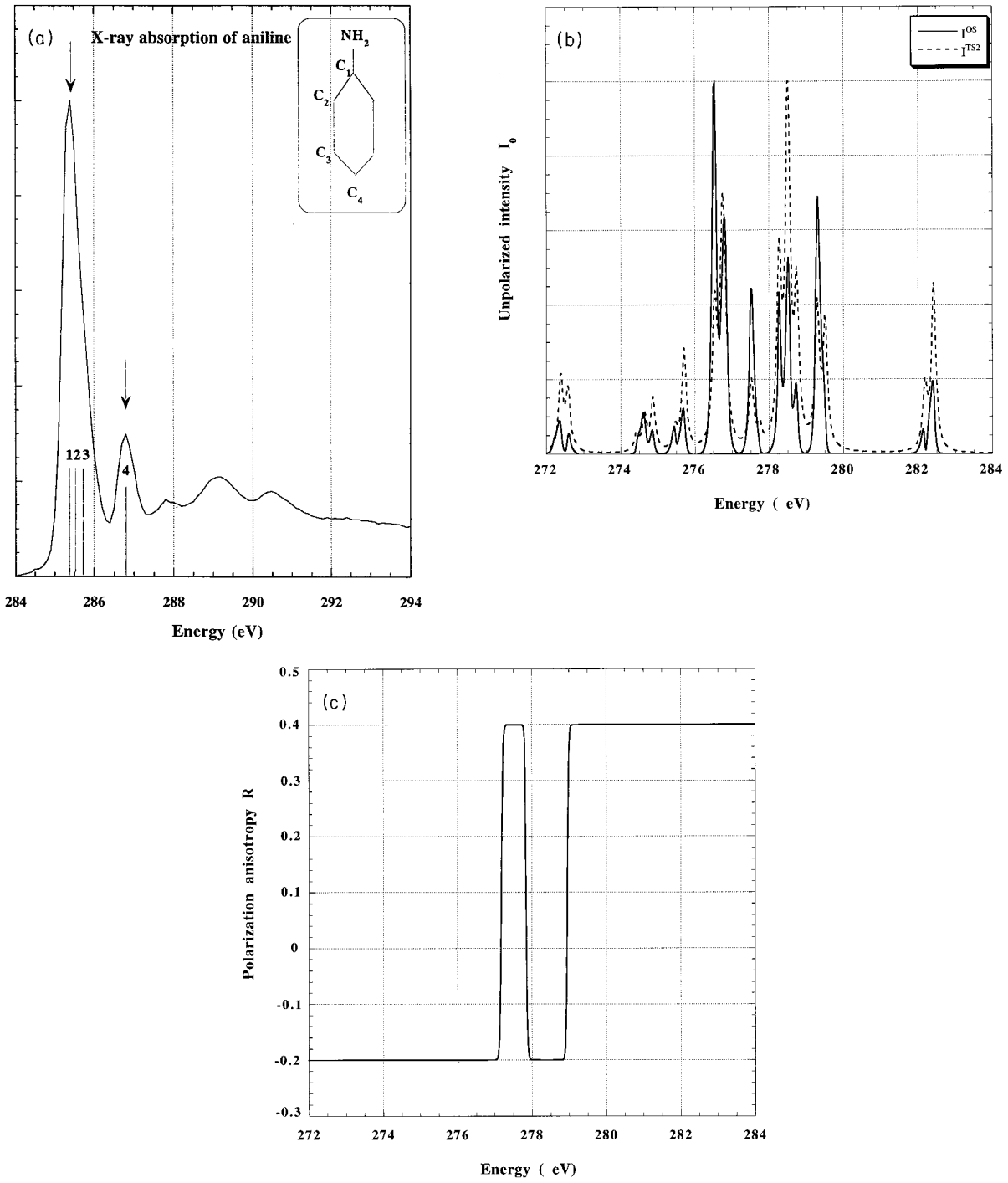

FIG. 3. Unpolarized intensity I_0 and polarization anisotropy parameter R for the aniline molecule. (a) X-ray absorption spectrum of aniline [22]. The corresponding assignments in the spectrum are (1) $C_2(a_1)\pi^*(b_1)$; (2) $C_3(a_1)\pi^*(b_1)$; (3) $C_4(a_1)\pi^*(b_1)$, and (4) $C_1(a_1)\pi^*(b_1)$. (b) I_0 calculated by one-step (solid line) and two-step (dashed line) models. (c) R.

level (t_{1u}) of C_{60}. Since there are a large number of symmetry adapted core orbitals involved in this process, the interference effect produces results from the one- and two-step models that are different for both I_0 and R; see Figs. 4(a) and 4(b). There are large differences especially for the polarization anisotropy. This implies that the polarizations ratios [8], which define much of the utility of RIXS in terms of symmetry assignment and orientational probing, also are completely different in the one- and the two-step models. If tail excitation and vibronic coupling are taken into account, we nevertheless believe that the actual differences will be diminished for the higher resonant states with more nonresonant appearance in the spectra.

The C_{60} species brings up the linking of the localized and delocalized descriptions of RIXS with the one- and two-step descriptions. As we have shown recently [7], the scattering channel interference depends strongly on the representation of the core excited states $|k^{-1}\nu\rangle$. For example, the interference vanishes strictly in the case of homonuclear diatomic molecules going from the localized to the delocalized repre-

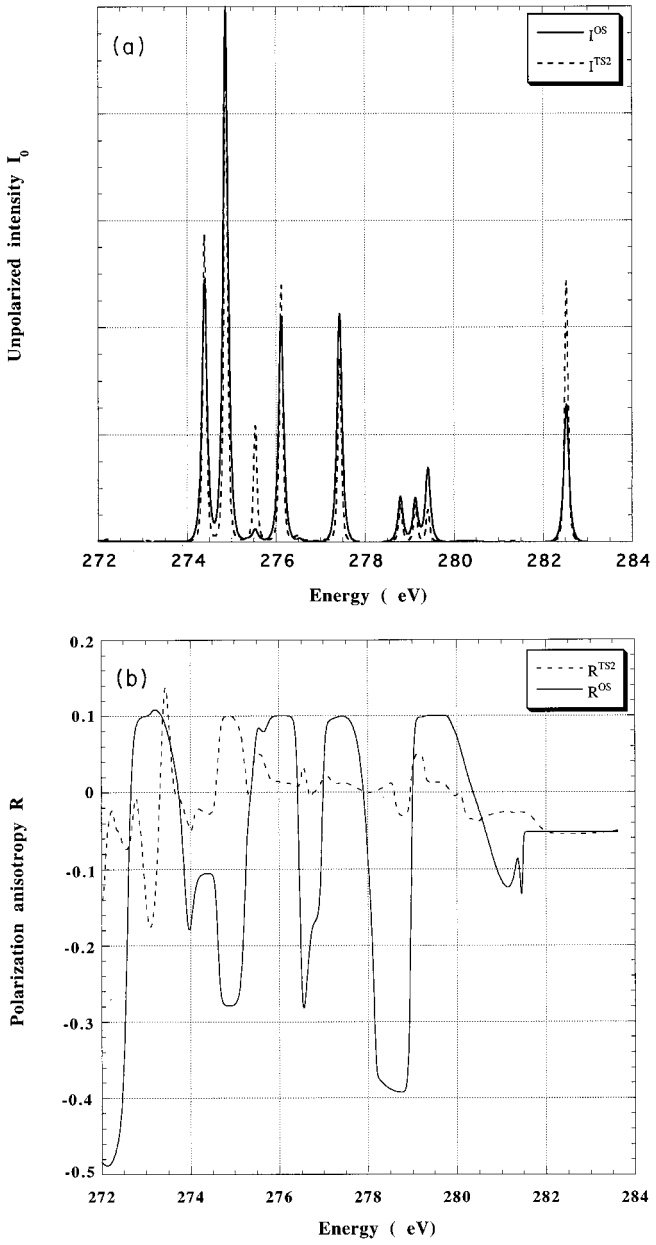

FIG. 4. (a) Unpolarized intensity I_0 and (b) polarization anisotropy parameter R for the C_{60} molecule, calculated by one-step (solid line) and two-step (dashed line) models.

sentations of core orbitals. However, the selection rules and the particular symmetry of the final state reduce the number of interfering channels in the symmetry-adapted representation for core states. The present simulations of C_{60}, CF_2Cl_2, and $C_6H_5(NH_2)$ seem to indicate that it is not possible to remove the interference in the general case by appropriate transformations of the intermediate states (as also indicated by the model example for C_{2v} symmetry given above). In the case of C_{60} the interference terms thus do not disappear under the transition from localized to symmetry-adapted representations of the core states, but this term influences strongly the shape, the total cross section, and the polarization anisotropy of the RIXS spectra. Thus we find the two-step model to be inadequate for the localized representation of the core states.

IV. SUMMARY

We have explored the consequences of the one-step formalism and the simplifying two-step and classical formulas for the polarization anisotropy in resonant x-ray scattering of randomly oriented molecules. The most important distinction between the one-step and two-step models is that the effect of x-ray *channel interference* is fully included in the former. This effect takes place when the intermediate core-excited states are coherently excited. The x-ray scattering channels defined by these different core-excited states will interfere when the energy gaps are of the same order of magnitude as the lifetime broadening. Investigations of the role of channel interference have previously been carried out for various other quantities, such as total cross sections for x-ray scattering in solids [23], vibronic fine structure in nonresonant x-ray spectra of molecules [10,24–26], multiple structures of x-ray excited states [27], and near-degenerate or chemically shifted core levels in resonant x-ray spectra [22].

It has previously been predicted that channel interference may lead to a strong dependence of the shape of the x-ray fluorescence spectrum on the frequency ω and on the polarization vectors of initial and final photons [7]. In the present work we quantified these predictions in terms of the one- and two-step formulations for the polarization anisotropy. The set of investigated molecules CF_3Cl, CF_2Cl_2, $C_6H_5NH_2$, and C_{60} covers the following four different situations: (i) when the two-step formula is applicable for both the unpolarized cross section I_0 and the polarization anisotropy R, (ii) when it is applicable for I_0 but not for R, (iii) when it is applicable for R but not for I_0, and (iv) when the two-step formula cannot be applied for either I_0 or R. The first case, for which also the classical formula for the polarization anisotropy is applicable (then identical to the two-step formula), covers the important class of molecules with energy isolated and symmetry nonadapted core hole states, for which the spectral analysis thus becomes much simpler than for cases (ii), (iii), or (iv). In case (i) [as well as in case (iii)] the symmetry assignments can be made using information of linearly polarized light only, while the other cases in principle require circularly polarized light to achieve that goal [8]. Calculations in case (i) lead to simple rational numbers for the polarization anisotropy depending only on symmetry and do not require energies and lifetimes as input, as when interference effects are important. The two cases (ii) and (iii) both represent large sets of common molecules, for which the two-step model is thus found inadequate. The reason that the two-step model is valid for I_0 but not for R in case (ii), and vice versa for case (iii), could be derived from the equivalence or inequivalence of the two-step model with the general one-step formulas (23) and (22) for the cross section and polarization anisotropy, respectively. The final case of high-symmetry molecules, case (iv), here illustrated by the C_{60} molecule, represents a smaller class of molecules, but is nevertheless interesting from the point of view of the symmetry and parity selective character of the x-ray scattering process. It can be noted that just those molecules for which the symmetry and parity selective character of the x-ray scattering is most relevant is at the same time the ones that are the most complex with respect to the interference effects and requirement of a full one-step implementation for both the polariza-

tion anisotropy and the integrated unpolarized cross sections.

The present findings can be of relevance for the use of the polarization anisotropy also for orientational probing of fixed oriented molecules. Surface adsorbates are systems with fixed or partially fixed orientations but, when physisorbed, have the simplicity in the organization of the unoccupied levels as that of free molecules and should be relevant samples for measurements of polarization anisotropies. More complex molecules and solids have a larger density of unoccupied states, which leads to stronger overlap of the core-excited resonances. This implies that interference will be more important also in case (i) despite that the bare core holes are isolated in energy. It might therefore be more difficult to extract symmetry information and to find simple relations between polarization ratios and symmetry or geometric properties for such samples and each case would probably require a full simulation. This should, in any case, be investigated further.

ACKNOWLEDGMENT

This work was supported by the Swedish Natural Science Research Council (NFR).

[1] P.L. Cowan, in Proceedings of the Ninth International Conference on Vacuum Ultraviolet Radiation Physics, edited by D.A. Shirely and G. Margaritendo [Phys. Scr. **T31**, 112 (1990)].
[2] R. Mayer, D.W. Lindle, S.H. Southworth, and P.L. Cowan, Phys. Rev. A **43**, 235 (1991).
[3] S.H. Southworth, D.W. Lindle, R. Mayer, and P.L. Cowan, Phys. Rev. Lett. **67**, 1098 (1991).
[4] D.W. Lindle, P.L. Cowan, T. Jach, R.E. LaVilla, R.D. Deslattes, and R.C.C. Perera, Phys. Rev. A **43**, 2353 (1991).
[5] J. Nordgren, P. Glans, and N.D. Wassdahl, Phys. Scr. **T34**, 100 (1991).
[6] F. Kh. Gel'mukhanov and L.N. Mazalov, Opt. Spektrosk. **42**, 659 (1977) [Opt. Spectrosc. (USSR) **42**, 371 (1977)].
[7] F. Kh. Gel'mukhanov and H. Ågren, Phys. Rev. A **49**, 4378 (1994).
[8] Y. Luo, H. Ågren, and F. Kh. Gel'mukhanov, J. Phys. B **27**, 4169 (1994).
[9] F. Kh. Gel'mukhanov and H. Ågren, Phys. Rev. A **50**, 1129 (1994).
[10] F. Kh. Gel'mukhanov, L.N. Mazalov, and N.A. Shklyaeva, Zh. Éksp. Teor. Fiz. **69**, 1971 (1975) [Sov. Phys. JETP **42**, 1001 (1975)].
[11] T. Åberg, Phys. Scr. **21**, 495 (1980).
[12] T. Åberg and B. Crasemann, in *X-Ray Resonant Scattering*, edited by G. Materlik, K. Fischer, and C. Sparks (Elsevier, Amsterdam, 1993).
[13] J. J. Sakurai, *Advanced Quantum Mechanics* (Addison-Wesley, Reading, MA 1967).
[14] F. Kh. Gel'mukhanov, L.N. Mazalov, and A. V. Kondratenko, Chem. Phys. Lett. **46**, 133 (1977).
[15] W. M. McClain, J. Chem. Phys. **55**, 2789 (1971).
[16] Y. Luo, H. Ågren, F. Kh. Gel'mukhanov, J.H. Guo, P. Skytt, N. Wassdahl, and J. Nordgren, Phys. Rev. B **52**, 14 479 (1995).
[17] D.W. Lindle, P.L. Cowan, R.E. LaVilla, T. Jach, R.D. Deslattes, B. Karlin, J.A. Sheehy, T.J. Gil, and P.W. Langhoff, Phys. Rev. Lett. **60**, 1010 (1988).
[18] S. Aksela, E. Kukk, H. Aksela, and S. Svensson, Phys. Rev. Lett. **74**, 2917 (1995).
[19] P. Skytt, J.H. Guo, N. Wassdahl, J. Nordgren, Y. Luo, and H. Ågren, Phys. Rev. A **52**, 3572 (1995).
[20] R.C.C. Perera, P.L. Cowan, D.W. Lindle, R.E. LaVilla, T. Jach, and R.D. Deslattes, Phys. Rev. A **43**, 3609 (1991).
[21] R.C.C. Perera, R.E. LaVilla, P.L. Cowan, T. Jach, and B. Karlin, Phys. Scr. **36**, 132 (1987).
[22] Y. Luo, H. Ågren, J.H. Guo, P. Skytt, N. Wassdahl, and J. Nordgren, Phys. Rev. A **52**, 3730 (1995).
[23] F. Kh. Gel'mukhanov, L.N. Mazalov, and N.A. Shklyaeva, Zh. Éksp. Teor. Fiz. **71** 960 (1976) [Sov. Phys. JETP **44**, 504 (1976)].
[24] F. Kaspar, W. Domcke, and L.S. Cederbaum, Chem. Phys. Lett. **44**, 33 (1979).
[25] A.F. Flores, N. Correia, H. Ågren, L. Pettersson, M. Bäckström, and J. Nordgren, J. Chem Phys. **83**, 2035 (1985).
[26] T.X. Carrol, S.E. Anderson, L. Ungiez, and T.D. Thomas, Phys. Rev. Lett. **58**, 867 (1987).
[27] A. Cesar and H. Ågren, Phys. Rev. A **45**, 2833 (1992).